

Original Article

Path Planning and Gait Analysis of Quadruped Robots

PVS Subhashini¹, Yemmanur Varun², Rohan Tadem³, G. Vanya Sree⁴, B.Venkata Siva⁵

^{1,2,3}Department of Mechanical Engineering, Vasavi College of Engineering, Hyderabad, India.

⁴Department of Mechanical Engineering, CVR College of Engineering, Hyderabad, India.

⁵Department of Mechanical Engineering, Narasaraopeta Engineering College, Narasaraopet, India.

¹Corresponding Author : pvs.subhashini@staff.vce.ac.in

Received: 20 February 2026

Revised: 28 March 2026

Accepted: 27 April 2026

Published: 29 May 2026

Abstract - Based on product production needs, various types of plant layouts are available in manufacturing. One such layout is the fixed-position layout, where assembly operations take place at a specific location, with components being delivered to that location. This paper shows the design of an automation-oriented quadruped robot used for transporting materials over uneven ground to deliver the parts to the fixed-position assembly zone. This paper gives a brief of the trajectory design, path planning, and gait analysis of a quadruped robot. The quadruped robot is modeled using SolidWorks CAD software. Its structural design was designed to ensure a balance of strength and practicality. Inverse kinematics have been effectively applied to this model, the relationship between joint configurations and the robot's legs, allowing for precise movement control. Trajectory planning was carried out, and path integration of the inverse kinematics equations was developed. Results are presented for various gaits, including walking, trotting, and galloping, which have confirmed the robot's capacity to adapt to various locomotion styles.

Keywords - Gaits, Inverse Kinematics, Motion, Path Planning, Quadruped robot.

1. Introduction

A legged robot is a type of robotic system that is specialized to apply animal- and human-like locomotion abilities. Legged robots provide motion using articulated limbs, in contrast to wheeled and tracked robots. The advantage of using articulated limbs as a form of locomotion is in increased flexibility to terrain types. Of course, wheeled systems by default have difficulty traversing rough, slippery, uneven, rocky, or any type of extreme terrain - legged robots do not.

Some advantages of legged/walking robots versus wheeled robots are in terms of complex and unstructured environments, like staircases or rubble, which wheeled robots cannot handle in the same way. Wheeled robots are designed to handle predictable terrains like roads and sidewalks. Movement in situations like staircases, rubble, mass debris, or steep inclines requires some adjustments to motion tracking or loss of contact with the ground, and movements of wheel-following robots would fail if there were changes in terrain. Legged robots are able to maintain a close "attach" of their foot-to-ground contact and avoid losing traction by stepping over terrain during foot-to-ground contact. The ground results in a vulnerable degree of independence from control, which was met with slight resistance (i.e., rough). Legged robots achieve a different relationship with the ground - the actors in the motion (primarily for this paper, legs) can allow for foot placement as well as to retain as much traction as possible

under strange terrain conditions with cutras, other possible solids around the status quo (i.e., abrasive agents or differing surfaces altogether), which speaks to an added flexibility. Some terms of vehicle-robot locomotion via distances and probable distances- a variant to the previous sentence, thus did not imply following transactions, up-hill, and downhill. It is true to notice that the adaptation of movement and combinations of movement would not only remotely expand mobility in general, but invite role engagement within applications, disaster response, and military.

Even with their advantages, legged robots typically can be more complex, expensive, and less energy efficient than a wheeled robot; but the advancements being made in kinematic design, actuation, and control systems are eliminating these drawbacks, making legged robots a more viable option for these situations that fault wheeled systems. Though there is a lot of research in material handling of robotic systems, a clear research gap was observed in the development of surface adaptive, automation systems capable of material transport in fixed-position layouts. Limited work has been observed in integrating robust trajectory planning, path optimization, and gait adaptability in quadruped robots for industrial material delivery applications. Addressing this gap is essential to improve flexibility, efficiency, and automation in such manufacturing settings. Yunn-Lin Hwang et al. [1] elaborate on an RR robot's kinematic and dynamic analysis. This mainly aids understanding Newton's Euler method on an RR



manipulator and also directs the determination of the torque needed for each joint and the forces acting on each link. This document provides some knowledge related to the offline programming and simulation, which refers to the control system that is intended to execute the pre-defined trajectory. Sachin Oak et al. [2] lay down a new idea towards the leg design in which a 4-bar mechanism is added for the movement of the 2nd link (lower). This stood as an extension of the idea that, in the development of the leg, a 4-bar mechanism installation is planned. Another major takeaway was performing a semi-elliptical trajectory. Alarazah Hussein Abdulwahab et al. [3] assisted with the theory of the different gait mechanisms in the quadruped robots. It also accounts for the concepts of static and dynamic stability of the robots. One more takeaway was the elaborate comparison of the different-legged robots, which was useful to comprehend their specifications and properties.

B Sandeep et al. [4] explore both the kinematic and dynamic modeling of quadruped robots. It shows the DH Parameters, inverse kinematics, followed by the plots for the Jacobian as well. The paper also covers the mechanical design considerations, i.e., the torque calculations from the motor. Followed by this, this paper shows a detailed gait motion with neat diagrams for the movement of the quadruped robot with trajectory planning, followed by the MATLAB simulation. Gor, Mehul al. [5], was helpful in understanding the compliance of a robotic arm. The importance of the suspension system in the leg was demonstrated. It also helps to understand the torque estimation, the actuator systems, and the fabrication process involved. Also, the model developed was taken as a reference to develop our model. Ganjare et al. Xianbao Chen et al. [6, 7] show the path taken as reference for the path and show the kinematic model of the quadruped robots, and Xianbao Chen et al. [7] show an algorithm to overcome the failure of more than one actuator of the leg. Semini et al. [8] introduced the design of the quadruped robot HyQ2Max, which is hydraulically actuated and torque-controlled. The robot features a rugged mechanical design and high-performing hydraulic actuation, allowing for dynamic locomotion, including jumping and running.

A major contribution is the torque control at the joint level, which enables fine force control and leads to better interaction with difficult terrain. The system is experimentally validated to show better agility, stability, and load-carrying capabilities. Jinrong Zhang et al. [9] was helpful for the forward kinematics of the leg model and the work volume study of the leg. Also, it shows the simulation in ADAMS.G. Bledt et al. [10] presents the structure and control of MIT Cheetah 3, a rugged and agile quadruped robot. It is actuated by high-torque-density electric motors using a proprioceptive actuation principle, where the robot is able to feel its position and forces through its own sensors. The onboard computing system is based on an embedded PC (with a real-time Linux) for locomotion control and data logging, and the leg

controllers run at high frequency for smooth leg joint motions. It is charged by a 450Wh lithium-polymer battery, supporting untethered operation for approximately two hours. Kim and Belkadi [11] recently presented a new direction for quadruped robot development with the use of wearable electronics that allow configurable sensors and reconfigurable electronics on the robot's body with different sensors or functionality over time for improved adaptability and interaction. Their reconfiguration method improves adaptability through dynamic reconfiguration of sensing and routing of data, and provides enhanced perception and task-specific functionality without modifying physical properties or changing how the quadruped robot perceives the world.

Jiang et al. [12] presented a proof-of-concept study to develop a pneumatically powered quadruped robot with soft rigid samples with rotary joints that are a hybrid of compliant soft actuators and rigid structure to provide a lightweight robotic limb that can adapt each leg to the task. The soft actuators exhibited improved shock absorption and the ability to conform to the terrain. Based on experimental validation, the quadruped robot achieved stable locomotion while attenuating forces to reduce mechanical loading. The results showed that using hybrid joints creates better outcomes for dynamic quadrupedal movement tasks.

Fan et al [13] presented a broad review on quadruped robots, addressing several areas including structural design, control strategies, and autonomous capabilities of motion. The review comprises content on quadruped systems categorized based on the type of actuations and gait control architectures. The review captured the changing trends of evolving from motion that is manually controlled to intelligent autonomous robots and the discussion of trade-offs among stability, agility, and energy efficiency. The review underscored the importance of perception and planning, as highlighted for future development.

N.D. Weerakkodi Mudalige et al. [14] propose Hyper Dog, which used an open-source platform for a quadruped robot based on ROS2 and micro-ROS, but its scores were still lower than Jester Walker. It has 12 RC servo motors, driven by a PCA9685 PWM driver, an STM32F4 microcontroller, which controls the servo motors at a low level, and an NVIDIA Jetson Nano carries high-level processing ability. A real-time onboard IMU offers orientation and stabilization feedback. The robot is charged by an 8.4V Li-Ion battery, allowing it to operate for about 50 minutes per charge.

Shelke et al. [15] introduced a smart quadruped robot with basic locomotion and remote control capabilities. The design consists of servo motors for motion, a wireless control, and sensors for basic obstacles. The design of the study is to still have a cost-effective and easily constructed object to be used as either an education or a prototype. The experiments showed that there is a reliable walking motion and basic reaction to

local environment factors, revealing its potential for basic robotics. Y. Geva and A. Shapiro [16] describe a new quadruped robot design intended for research. The robot is constructed with an ArbotiXrobo controller, an AVR-based controller that has been designed specifically to control Robotis Dynamixel servo motors. The motors are accessed via an RX Bridge, and the system is wireless using XBee modules.

The robot has a 4S LiPo power source, with voltage levels regulated to avoid over-discharge. The design is Arduino IDE-compatible and open-source, allowing researchers to extend and modify the capabilities of the robot. Budanova et al. [17] showed MORS, a small quadruped robot controlled by Brushless DC (BLDC) motors; the robot was light and easily constructed with a modular design, and took advantage of BLDC efficiency and smooth motion compared to servos. The study's results were sound, so that kinematic analysis and initial tests were completed, stable gaits and navigation over flat terrain were successfully undertaken.

Y. Shi et al. [18] proposed structural design, simulation, and experiments on a quadruped robot. The robot uses an STM32 microcontroller based on a Free RTOS system for controlling locomotion and self-balancing functions. The actuation is provided by SCS0009 bus servos, allowing for accurate movement of its joints. There is also an onboard IMU sensor module to sense pitch and roll angles, helping to control real-time self-balancing. The electronic part is economical but provides stable performance for dynamic stability and gait planning.

A. Shahriar and M.H. Anik [19] present CHIGLU, a quadruped robot with a stepper motor and a modular hardware platform. The platform employs an Arduino Mega PRO microcontroller for low-level motor control and a Linux-based machine for motion planning and posture control. It combines DRV/TMC series motor drivers, AS5600 encoders for feedback on position, and various power regulation circuits to supply 12V, 9V, and 5V to various components. A power distribution network (PDN) analysis was done to confirm that voltage levels and current density on the board were correct, facilitating safe operation.

M. Hutter et al. [20] introduced ANYmal, a dynamically moving and mobile quadruped robot that can walk over challenging terrain. It is driven by torque-controlled electric motors and accommodates onboard sensors for state estimation and terrain adaptation. The control system of the robot can accommodate multiple locomotion gaits, such as trot and crawl. It has a modular structure that enables it to be deployed in the field, and it shows robust performance in unstructured outdoor environments.

Hamza Khan et al. [21] built a small hydraulic quadruped robot named MiniHyQ, which is completely torque controlled. Small-sized actuators are selected to build a small-sized

quadruped robot. Experiments are conducted on a MiniHyQ for design verification and testing on hardware.

Pablo et al. [22] performed a survey of quadruped walking machines, classifying past and current designs according to mechanical structure, actuation style, and gait generation. The research points out fundamental difficulties in leg coordination, efficiency in energy, and terrain adaptability, and offers a basic point of reference for the development of quadruped robots.

Sheng Dong et al. [23] present a thorough review of the adoption of effective algorithms for gait planning and provide access to theoretical references to the researchers working on quadruped robots.

Mauricio Becerra et al. [24] discussed about impedance controlled inverse dynamics within a locomotion control framework supported by trajectory tracking. MuJoCo is a popular virtual prototype reproducing real-time systems of robots. In this paper, the author simulated the dynamic effect on contact parameters of the controlled robot. Also presented videos, simulations of the controlled quadruped robot, and presented the effects of contact parameter values on contact dynamics.

Jessy W. Grizzle et al. [25] proposed the Hybrid Zero Dynamics (HZD) approach to control legged robots. Although initially used for biped robots, the technique is transferable to quadrupeds to synthesize stable periodic gaits. It formulates legged locomotion as a hybrid dynamical system and employs feedback control to achieve trajectory invariance between discrete and continuous phases.

2. Methodology

The kinematic structure of the robot arm in an RRR configuration is defined by its three rotational joints, which allow for precise angular movements in a workspace. Initially, will be working only on the planar RR, i.e., linear movements of the robot. This configuration provides flexibility and simplicity, making it ideal for designing a simple quadruped robot's core.

The analysis of this structure involves determining the forward and inverse kinematics to establish a clear relation between joint angles and the desired position of the end effector. Trajectory will be derived for the motion of the quadruped robot and will be clubbed to the kinematics calculated, whose results will be later given as rotary input to the robot via appropriate motors.

The basic kinematic structure is an RR (planar) manipulator in a vertical orientation. One end is on the ground, and the other is connected to the torso via another revolute joint.

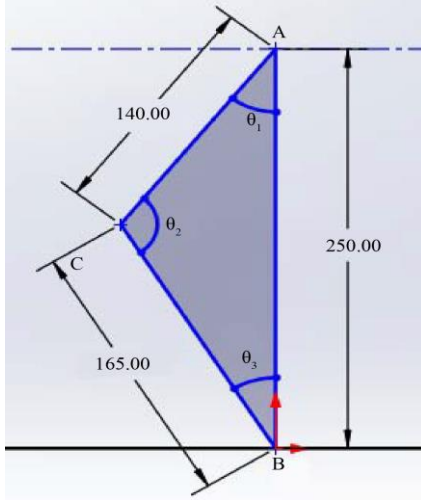


Fig. 1 Geometrical structure of the leg

The basic design was based on only the L2 and L3 links, i.e., a planar RR robot shown in Figure 1. This segment was well designed to reach the required parameters in terms of maximum step height of the robot, etc., and also the fact that it is the core of a quadruped robot. A ground clearance of 250mm was assumed, and the links were placed in an orientation by taking the following assumptions about the links.

- Link 1 Length = 140 mm
- Link 2 Length = 165 mm

These link lengths were the first iteration of the kinematic analysis since they sit comfortably fine for the assumed ground clearance. Also, due to torque multiplication, the length of link two is assumed to be more than that of link 2.

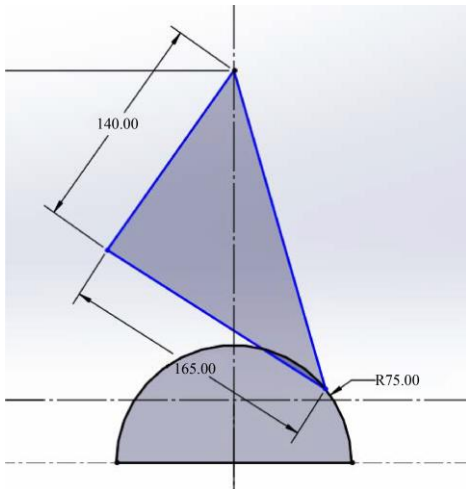


Fig. 2 Path and line diagram of the leg (Inverse Kinematics)

2.1. Inverse Kinematics

Inverse kinematics is a vital area of robotic motion planning. For the planar RR (2R) robot, a simplified planar representation of a quadruped leg, the inverse kinematics

problem is concerned with obtaining the required joint angles of the leg's end-effector (usually the foot) to achieve specific positions. Inverse kinematics is particularly important in trajectory planning for quadrupeds, where the quadruped robot needs to ensure stability and smooth motion while adjusting to gait changes and different terrains.

To begin, a line diagram and the proper notations to complete the kinematics on the geometry are drawn as shown in Figure 2.

By the cosine rule,

$$\Rightarrow \cos\theta_2 = \frac{a^2+b^2-c^2}{2ab} \quad (1)$$

$$\text{and } \theta_1 = \cos^{-1}\left(\frac{b^2+c^2-a^2}{2ab}\right) \quad (2)$$

Where, A, B, and C are the vertices of the triangle shown in the Figure.

$\theta_1, \theta_2, \theta_3$ are the corresponding angles at A, B, and C, respectively;

a, b, c are the lengths of sides opposite to A, B, C, respectively.

So, by using the cosine rule, the angle for theta 2 can be calculated straight away, and for theta 1, the following needs to be added.

$$\Rightarrow \theta_1^1 = \tan^{-1}\left(\frac{x}{y}\right),$$

$$\text{Hence, net } \theta_1 = -\tan^{-1}\left(\frac{x}{y}\right) + \cos^{-1}\left(\frac{b^2+c^2-a^2}{2bc}\right)$$

This is supposed to be clubbed with the trajectory planning equation, which is to be formulated according to the type of path that the leg is required to travel.

2.2. Energy and Torque Analysis of Leg Actuators

Energy efficiency has a significant role in the performance of the quadruped robot, especially during continuous gait cycles on different terrains. In relation to the robot proposed here, each leg can be represented as an RRR kinematic chain, for the majority of the motion in each leg will occur in the planar RR section, demonstrating varied swing and stance phases.

In order to obtain estimated actuator torque requirements, a simplified torque equation can be designed for each joint:

$$\tau_i = I_i * \alpha_i + m_i * g * r_i * \cos(\theta_i)$$

Where:

- τ_i : torque at joint i
- I_i : moment of inertia of the link
- α_i : angular acceleration
- m_i : mass of the link

- g: gravitational acceleration (9.81 m/s²)
- r_i: distance from joint to center of mass
- θ_i: angle of joint

For the MG996R servo motors used in the design, each had limits of torque values (nominal) of approximately 10 - 12 kg · cm (≈1.0 - 1.2 Nm). Based on the link dimensions:

- Link 1: 140 mm (0.14 m), Link 2: 165 mm (0.165 m)
- Estimated link mass of 0.2-0.3 kg per link

The results presented for the semi-circular showed that joint torques for the leg remained under 1.1 Nm, a joint torque well within the operational margin of the MG996R under typical walking gaits. In the more dynamic gaits, such as galloping, it is observed that more angular acceleration contributed to the maximum torques exceeding the limits for the servos. Compared to Bledt et al. [10] describing the MIT Cheetah 3, a very strong and torque-controlled dynamic quadruped robot operating autonomous and dynamic locomotion, the work put forth here is primarily focused on the design and simulation of a quadruped robot using SolidWorks. The work done by the MIT team with the Cheetah 3 has much more robust control strategies, including model-predictive control, real-time perception, developed actuator dynamics, and a complex design process. Compared with the strength of design and control development by MIT, this study emphasizes mechanical feasibility, modular design, and kinematic motion analysis within a simulation.

Different from Cheetah 3, which has been evaluated extensively in the real-world tackled environments, such as testing in rough terrains and autonomous times of operation, the work here is challenging the pre-fabrication phase with hardware availability and funding. Therefore, the work does not include physical, observable experimentation; however, the simulations offer good insight into structural behavior and offer a solid foundation for future prototyping.

Table 1. Power consumption comparison

Parameter	Hobby Servo Quad	MIT Cheetah
Motors	PWM servos	BLDCs with torque control
Peak Power (Walking)	~30-40 W	~300-600 W
Peak Current	~8-10 A	~30 A+
Battery Voltage	6-7.4 V (2S LiPo)	22.2 V (6S LiPo)
Battery Capacity	2.2-5 Ah	6-8 Ah

2.3. Trajectory Planning

The trajectory planning is an essential part of the configuration process of a quadruped robot. For the walking quadruped robot, this paper focused on trajectory planning of

the leg's endpoint (foot tip), which travels along a given path. A semi-circular curve is the preferred trajectory because of its simple structure and because it is naturally suitable for the imitation of human walking.

The term such a trajectory-producing scheme as a workspace end-effector trajectory, which is expressed mathematically as equations combined with the inverse kinematics of a robot. This noise-free integration permits the determination of the necessary joint angles of the leg to reproduce the wanted semi-circular path accurately, causing a precise and coordinated movement during the operation.

Generally, the shape is seen to be 2 sine waves, one under the other, the bigger amplitude sine wave being on the top of the x-axis and the smaller amplitude one being below. A rough shape is shown in Figure 3.

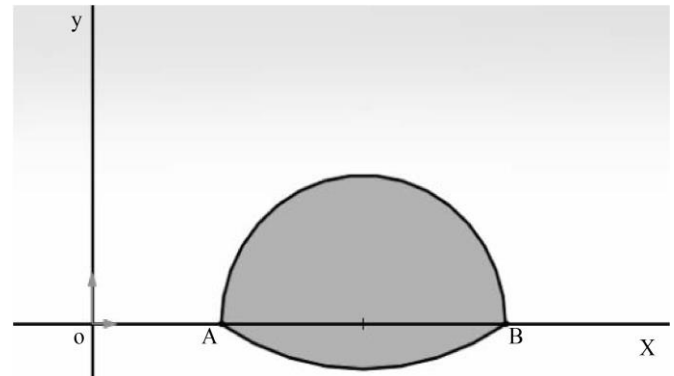


Fig. 3 Sine wave path of the end effector

Path ⇒ A → B → A

To simplify the equation/locus of the trajectory, the path in Figure 4 is assumed to be a semicircle as shown. The radius of the circle will determine the height of the obstacle that the robot will be able to walk over. This can be varied according to the situation, terrain, and speed.

The equation/locus for the trajectory is the equation of the circle itself, considering only the positive values of the y coordinate, assuming the center of the circle is on the x-axis. This equation would give a trajectory for the desired semi-circular path,

i.e. for $y \geq 0$, $x^2 + y^2 = r^2$.

To compute coordinates at each point of the trajectory to work out the inverse kinematics, add a for loop in the program and club it with the inverse kinematics code and the motor input interface.

for x in range (-r, r+1); $y = \text{sqrt.}(r^2 - x^2)$;
 $C_x = x$; $C_y = \text{ground clearance} - y$

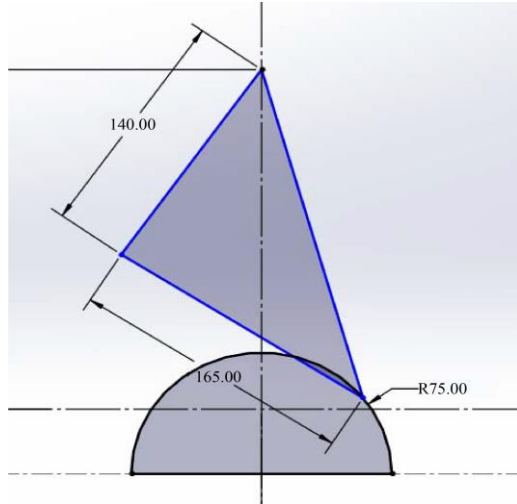


Fig. 4 Path and line diagram of the leg (Trajectory Planning)

By clubbing this with inverse kinematics equations, angles at each point in the trajectory can be obtained. And this input is given to the servo motors respectively. For clubbing,

replace the x and y coordinates of the trajectory equation with the inverse kinematics equation.

So, from the diagram, solving for the (75,250) point on the path, a=165; b=140; and C= distance b/w (0,0) and (75,250)

$$\text{Hence } \Rightarrow \cos\theta_2 = \frac{a^2+b^2-c^2}{2ab}$$

$$\Rightarrow \theta_2=117.450o$$

And,

$$\text{Net } \theta_1 = -\tan^{-1}\left(\frac{x}{y}\right) + \cos^{-1}\left(\frac{b^2+c^2-a^2}{2bc}\right) \text{ where } x=76, y=250$$

$$\text{Hence net } \theta_1 = 34.12 - 16.69 = 17.42o$$

To validate the calculations, a code is written on the same equation, which is given below, along with the result, which is validated from the Solid Works interface.

Table 2. Comparison of the above with various quadruped robots

Feature	Proposed Robot (Subhashini et al.)	MIT Cheetah 3 [10]	HyperDog [14]	CHIGLU [19]
Inverse Kinematics Approach	The analytical solution of a two-link RR planar manipulator combines the cosine rule and inverse kinematics to track semi-circular paths.	A model-based control system implements dynamics through the use of high-frequency control loops along with proprioceptive feedback.	Basic kinematics for hobby servos; Controlled via PWM with limited sophistication around IK	Modular design; stepper motors have simple kinematics, so they can be used for educational use
Gait Efficiency and Stability	Simulated different gaits: walk, trot, pace, and gallop, with gait parameters such as phase difference and duty cycle calculated; semi-elliptical path to clear obstacles.	High dynamic stability via real-time torque or power control; good for rough terrain	Mild gait stability; uses IMU for feedback; low terrain adaptability	Basic gaits for locomotion, defined for controlled environments, have low gait adaptability
Computational Complexity of Path Planning	Low to moderate; defined semi-circular trajectory; angles computed per step using basic geometry loops.	Control bandwidth is high; it has an onboard real-time operating system and embedded control with trajectory optimization.	Moderate; Jetson Nano uses ROS2-based motion planning	Low-level; Arduino-based path logic; only has path execution

2.4. Modelling

Here, the links lie one behind the other, joined by the motor cap attached to the upper link. The motor for the second link is placed on the link itself as follows.

Figure 5 shows that the upper link is of length 140 mm with a thickness of 20 mm to satisfy the clearances. The width at the center is 40 mm, leaving 5-7 mm clearance at each end for the caps, respectively.

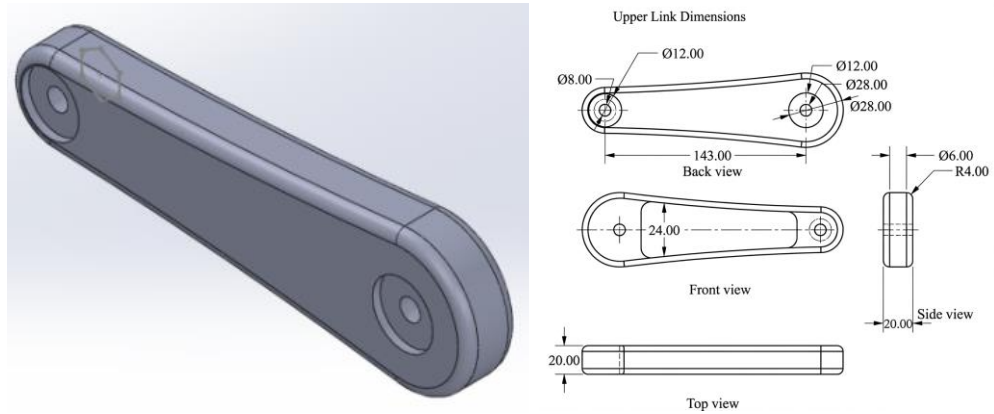


Fig. 5 Upper Link Dimensions

The lower link is designed in a similar way to the upper link. It is of the length 165 mm and with a thickness of 20 mm. Grooves are made for the motor caps on the links at both ends.

Additionally, there is a ball attached to the bottom of the leg, preferably made of rubber, to gain more friction and control on the ground while moving, which is represented in Figure 6.

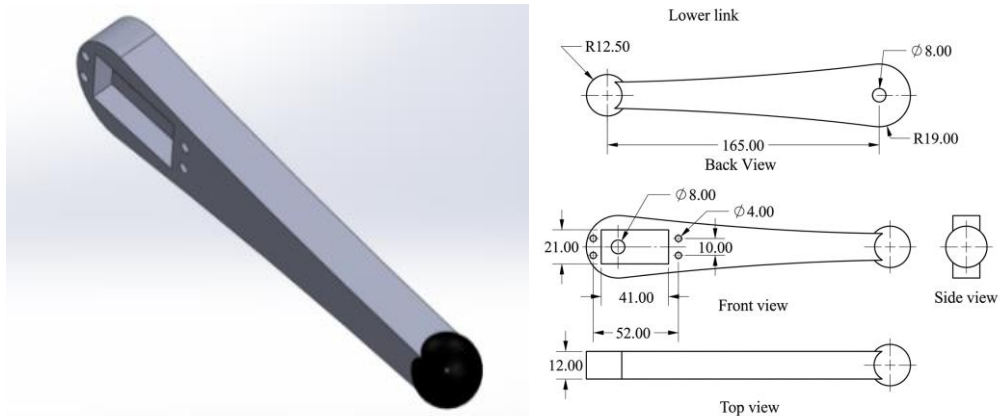


Fig. 6 Lower Link Dimensions

The motor grooves are done for the MG996R and MG995 servo motors in this design specifically. Figure 7 shows a torso plate which is designed to incorporate all the working components of the robot, which includes servo motors, battery

pack, microcontroller (any appropriate microcontroller), clearance for the 4 legs, and any other fancy sensors. The torso design shown is a raw design that will only cater to the minimum requirement.

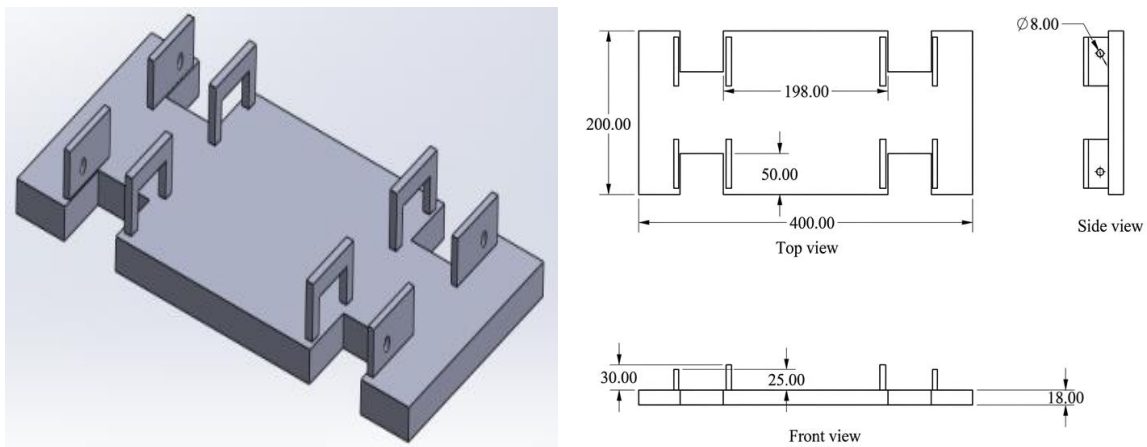


Fig. 7 Dimensions of Torso

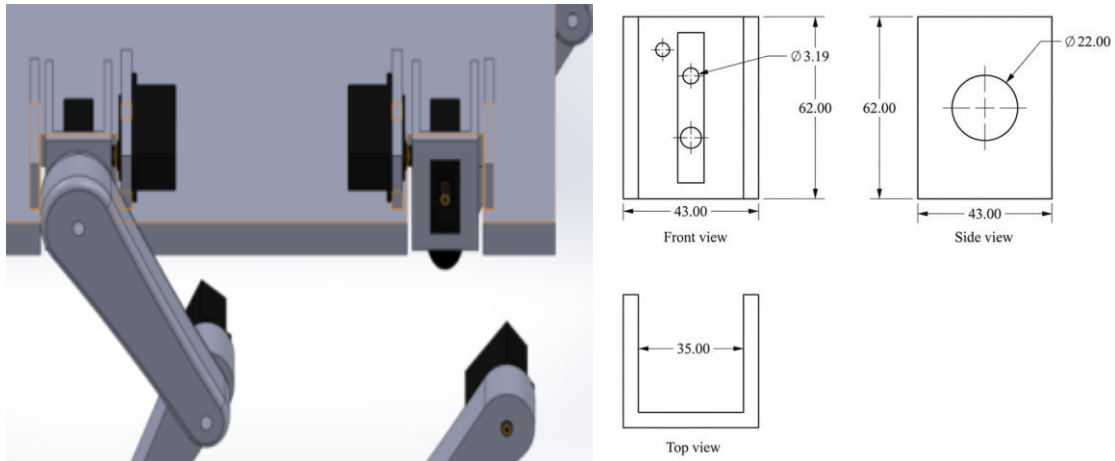


Fig. 8 Dimensions of the Connector

This is the link that is moved along the axis across the surface of the torso. This helps the robot to turn. Hence, a similar servo motor is placed on the grooves shown and is actuated according to the situation. This link is set up pivoting about 2 points, i.e., the servo motor shaft and the bolt. This servo motor is attached to the extrusion given on the torso plate with bolt provision, as shown in Figure 8.

2.5. Gaits in Quadruped Animals

Gaits are defined as the particular patterns of limb movement a quadruped robot has for moving about. Gaits allow a legged robot to perform walking, running, or trotting tasks efficiently, robustly, and adaptively in various terrains

and while executing various tasks. Good gait design provides stability as the weight of the robot is balanced at any point, regardless of needing to accommodate uneven ground or changing direction quickly. Gaits offer better energy efficiency, which is significant if the robot needs to work on a limited energy budget.

Quadruped robots can do a number of different gaits, which are usually classified based on duty factor (the proportion of time a leg is in contact with the ground during a gait cycle) and phase offsets of the legs. There can be a number of gaits; however, this paper is only considering the set of walking, trotting, pace, and gallop.

2.5.1. [A] Various Types of Gaits

Table 3. Input variables for the motion simulation

Action	Pattern	Limb Movement	Speed	Energy Efficiency	Purpose	Examples
Walk	An asynchronous motion with three legs engaging the ground surface for stability	Sequence of left hind limb→left front limb→right hind limb→right front limb	Slow	Very energy efficient and stable	Slow, steady, hopefully - nothing will disturb. For grazing and exploration purposes	Cows grazing in a field, elephants walking.
Trot	diagonal paired limbs move together (e.g., left front and right hind, then right front and left hind).		Faster than a walk, slower than a gallop.	Efficient and can be used for greater distances.	Slightly faster locomotion.	Dogs trotting, horses transitioning gait from walk to a canter.
Pace	Lateral paired limbs move together (e.g., left front and left hind, then right front and right hind).		Moderate; similar in speed to trot.	Less efficient, but there is a reason some animals pace, like anatomical advantages.	The use of animals with long legs or slender body types mitigates limb interference patterns.	Camels, giraffes.

Gallop	A four-beat gait where the legs move in a sequence, with a suspension phase where all four legs are in the air.		Less efficient	Less efficient	Used for high-speed running, such as hunting or escaping predators.	Cheetahs sprinting for prey, horses racing on a track.
--------	---	--	----------------	----------------	---	--

2.5.2. [B] Properties of Gaits

Table 4. Input variables for the motion simulation

Properties	Definition	Formula
Phase Difference	Phase difference is the time or angular offset between the movements of the two legs within the gait cycle. Typically shown as a proportion or percentage of the gait cycle.	$\phi = \frac{\Delta T}{T(\text{Cycle})}$ Where ϕ is the phase difference ΔT is the time difference between the corresponding events (eg, lift-off or touch-down) of each leg. $T(\text{Cycle})$ is the duration of one full gait cycle.
Duty Cycle	Duty cycle is the proportion of the gait cycle that a leg is on the ground (stance phase). It is a measure of stability and expressed as a ratio or percentage.	Duty cycle = $(T(\text{Stance})) / (T(\text{Cycle}))$
Stance Time	Stance time is the duration that a leg is in contact with the ground within a gait cycle.	$T_{\text{Stance}} = \text{Duty Cycle} \times T_{\text{Cycle}}$
Swing Time	Swing time is the duration that a leg is off the ground and moving to its next position in the gait cycle.	$T_{\text{Swing}} = T_{\text{Cycle}} - T_{\text{Stance}}$

Table 5. Input variables for the motion simulation

Gait	Phase Difference(sec)			
	Right Front	Right Rear	Left Front	Left Rear
Walk	0	0.69	1.38	2.07
Trot	0	1.38	1.38	0
Gallop	1.38	0	1.38	0
Pace	0	0	1.38	1.38

in its plane for all the 4 legs and a path mate is given for the leg point and a path. Then, the path mate is given with a path motor and the inputs for each motion and the time interval. Constant velocity is not given to demonstrate real-life scenarios, as the starting and ending of a stride cycle are relatively low. are given according to the calculations done previously.

2.6. Motion Study

The motion study is done in SolidWorks, and the plots are generated in the same software for the gaits. To start with, the path for each end effector point is already drawn as a sketch

The input given is the total distance travelled by the end point without and with phase difference, which are shown in Figures 9 and 10, respectively.

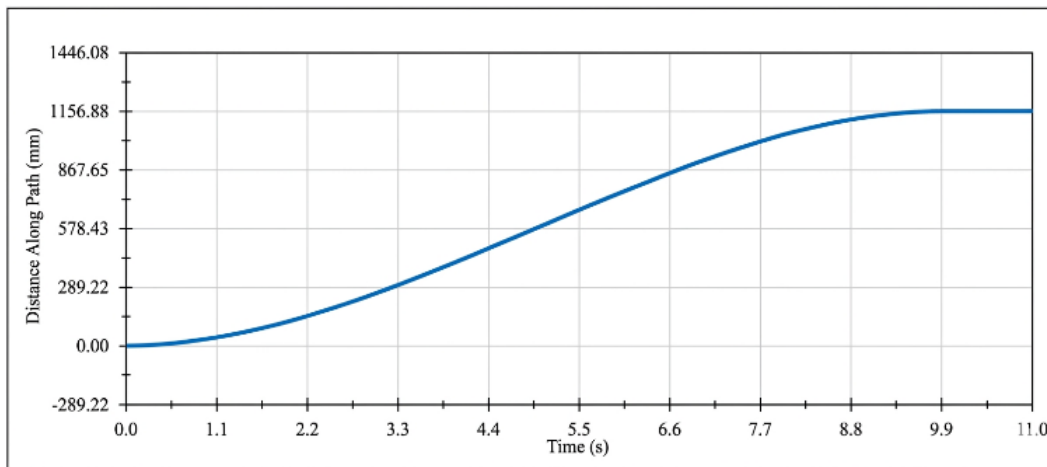


Fig. 9 Distance v/s time plot without phase difference

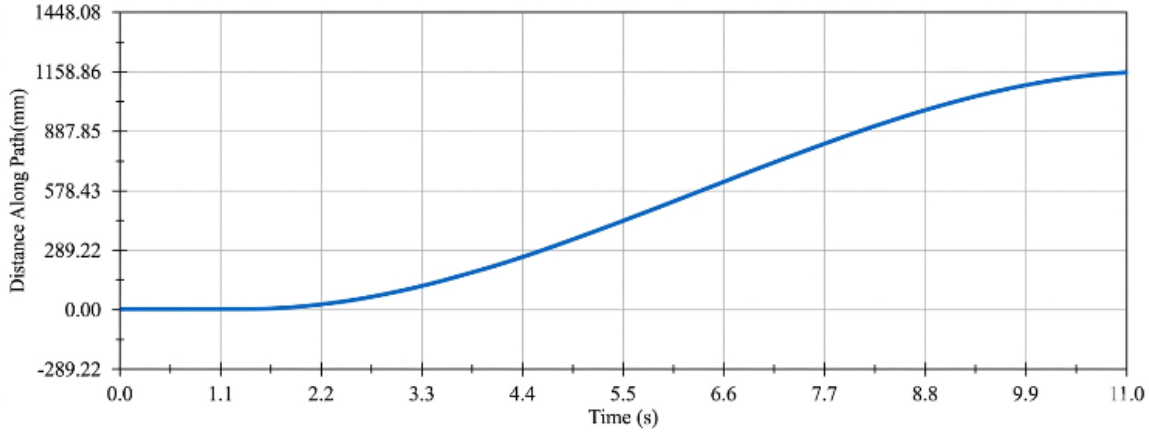


Fig. 10 Distance v/s time plot with phase difference

3. Results and Discussion

3.1. A graphical Representation of the Walk is Given Below

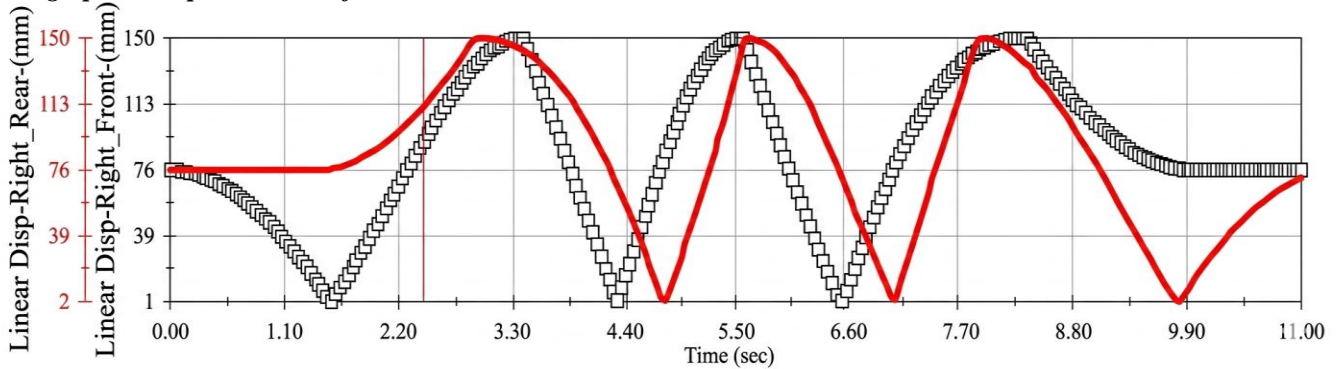


Fig. 11 Linear displacement vs time graph between the right front and the right rear

From Figure 11, it is observed that each leg starts after an interval of 1.38s (phase difference), starting from the right rear with respect to linear displacement. It can be seen that each

leg starts after an interval of 1.38s (phase difference) Starting from the right rear, with respect to linear velocity, can be observed in Figure 12.

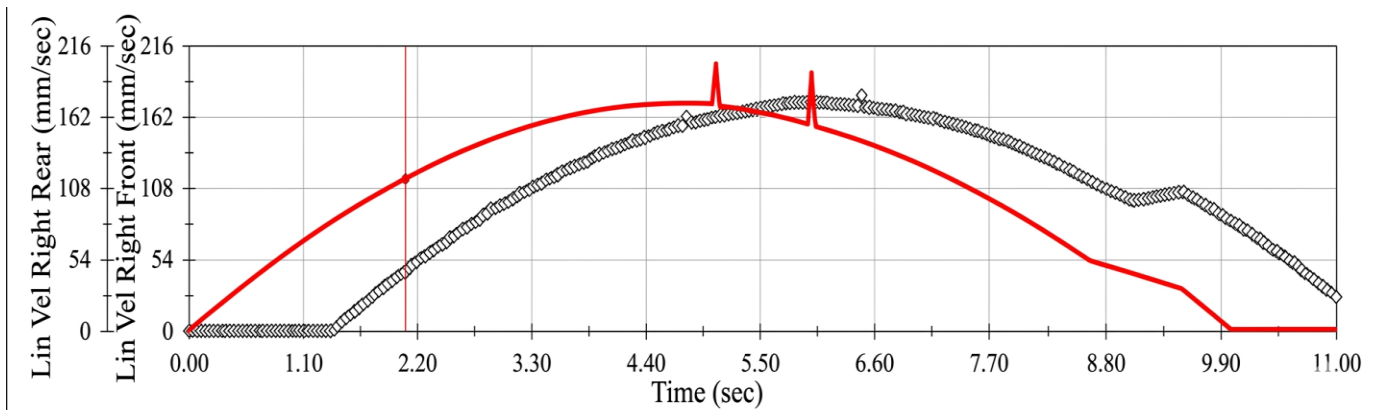


Fig. 12 Linear velocity vs time graph between the right front and right rear

The phase difference can be seen clearly in the graph, and it is for the right front and right rear legs; the same trend would continue with left front followed by left rear leg in Figure 13. In Figure 14, it can be seen that the right front and left rear move together and are in a phase difference from the other 2

legs with respect to angular displacement. It can be seen in Figure 15 that the right front and left rear move together and are in a phase diff from the other 2 legs with respect to linear velocity.

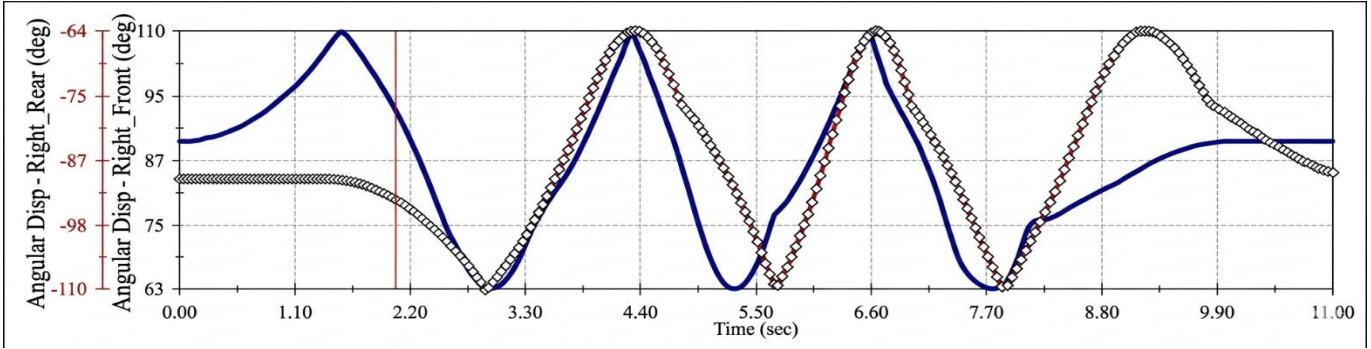


Fig. 13 Angular displacement vs time graph between the right front and the right rear

3.2. Graphical Representation of Trot is Given below

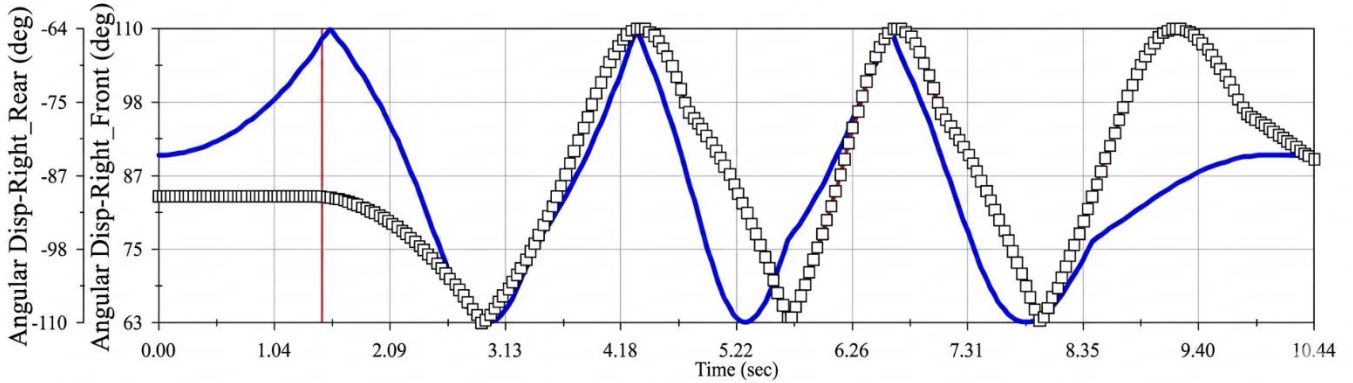


Fig. 14 Angular displacement vs time graph between the right front, left, and rear

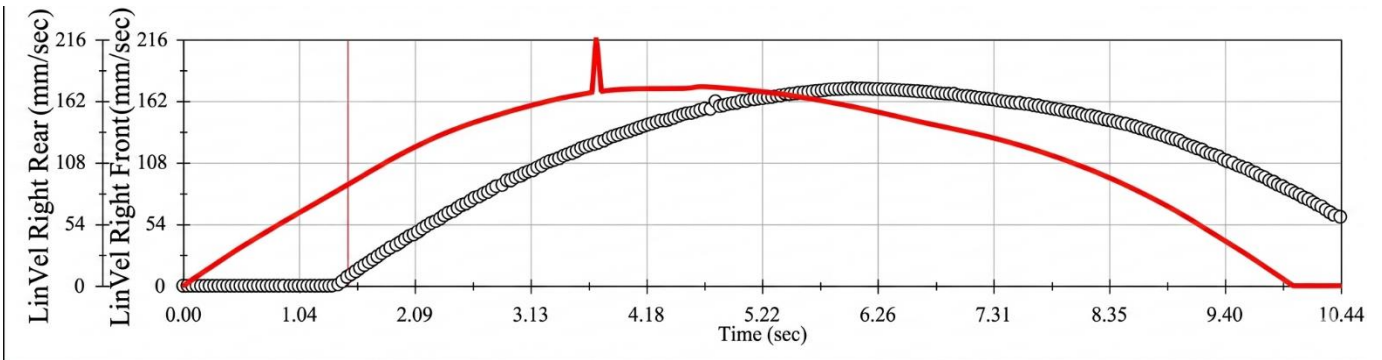


Fig. 15 Linear velocity vs time graph between the right front and the left rear

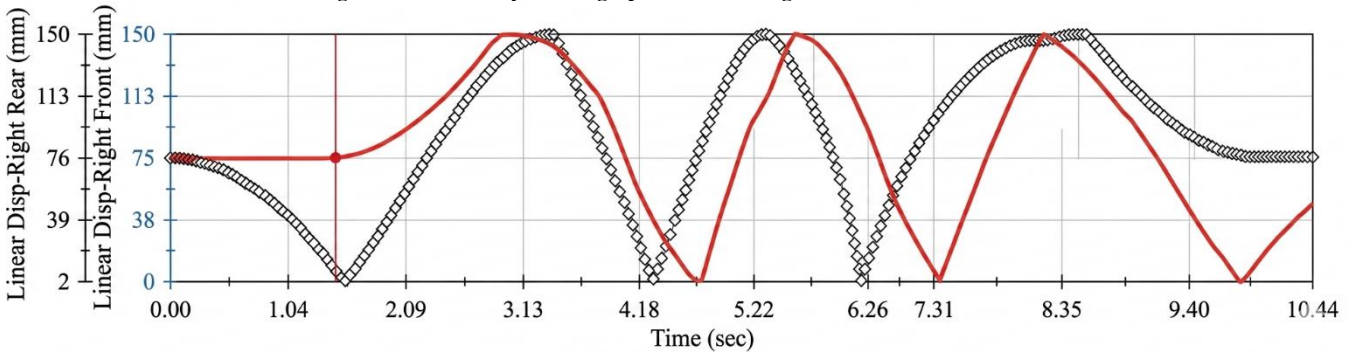


Fig. 16 Linear displacement vs time graph between the right front and the left rear

As the phase difference can clearly be observed in Figure 16. The diagonal legs move together, followed by a phase difference in the next pair of diagonal legs.

3.3. Graphical Representation of Pace is Given Below

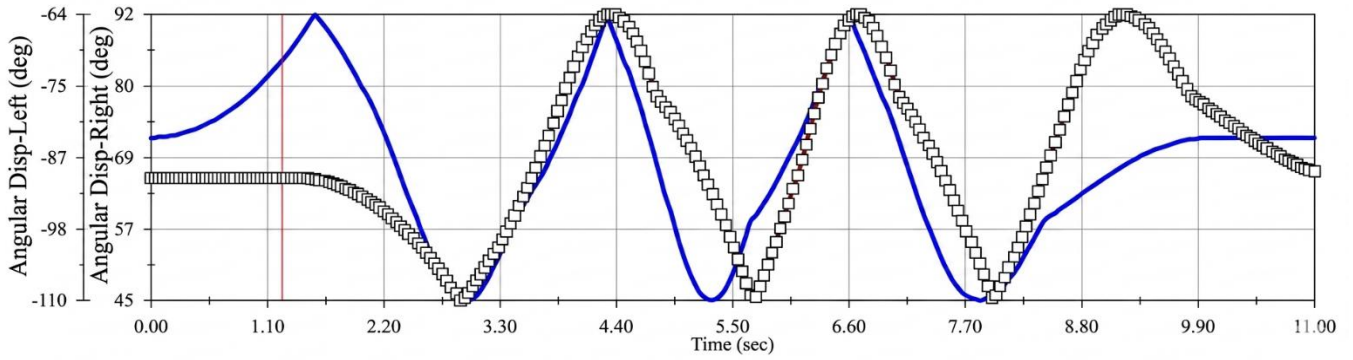


Fig. 17 Angular displacement vs time graph between any right and any left leg

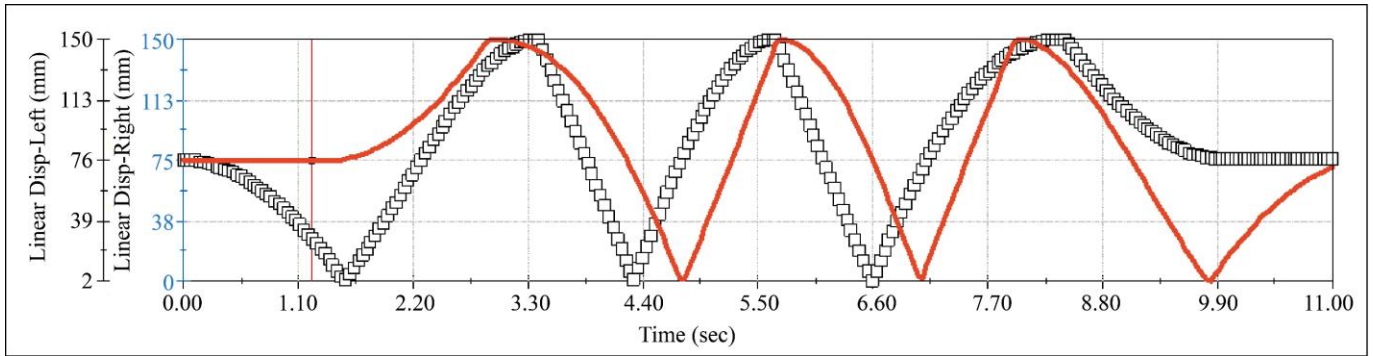


Fig. 18 Linear displacement vs time graph between any right and any left leg

From Figure 18, it can be seen that both right legs move together and the left ones move together. As the phase difference can clearly be seen in Figure 19, the same side legs move together, followed by a phase difference on the next side of the legs.

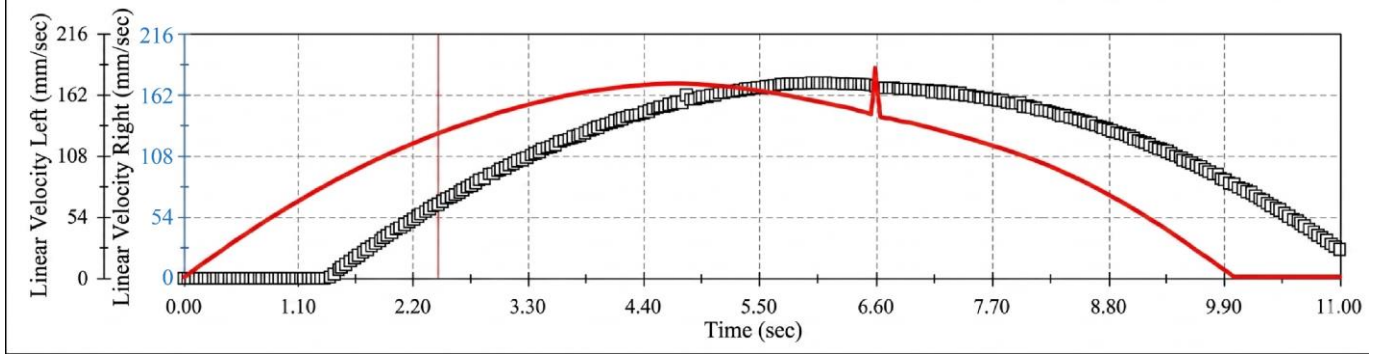


Fig. 19 Linear velocity vs time graph between any right and any left leg

3.4. Graphical Representation of Gallop is Given below

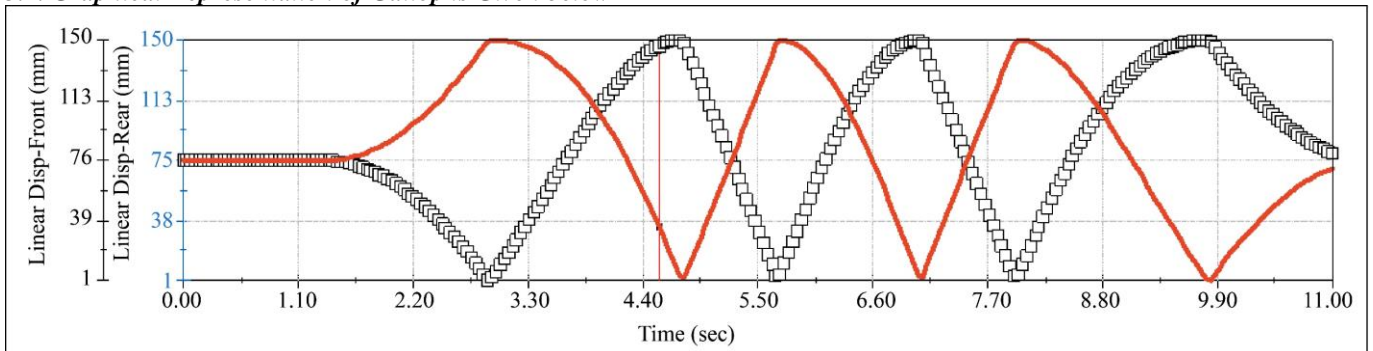


Fig. 20 Linear displacement vs time graph between front and rear legs.

It can be seen that the rear legs move together and the front ones move together, with a phase difference of 1.38s, as shown in Figure 20.

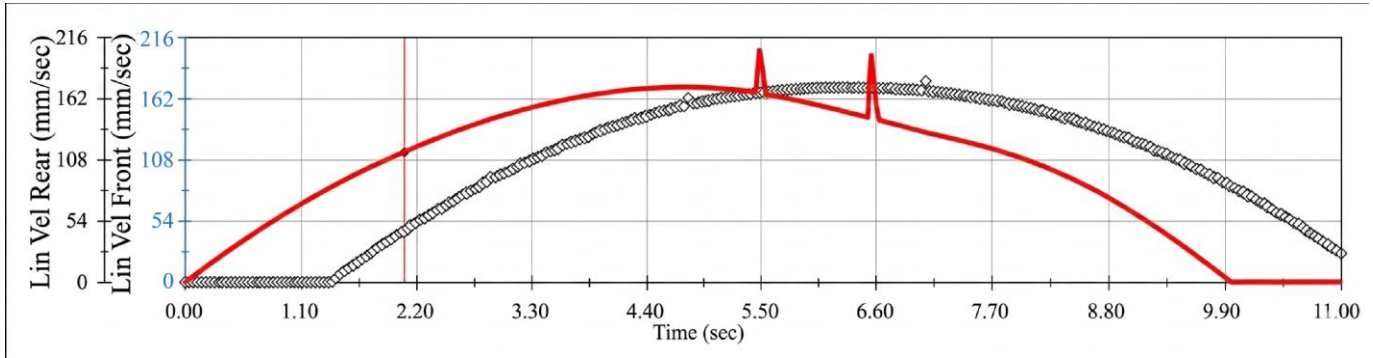


Fig. 21 Linear velocity vs time graph between front and rear legs

From Figure 21, it can be seen that the rear legs move together and the front ones move together with a phase difference of 1.38s. As the phase difference can clearly be seen in Figure 22, the rear legs move together, followed by a phase difference in the front legs.

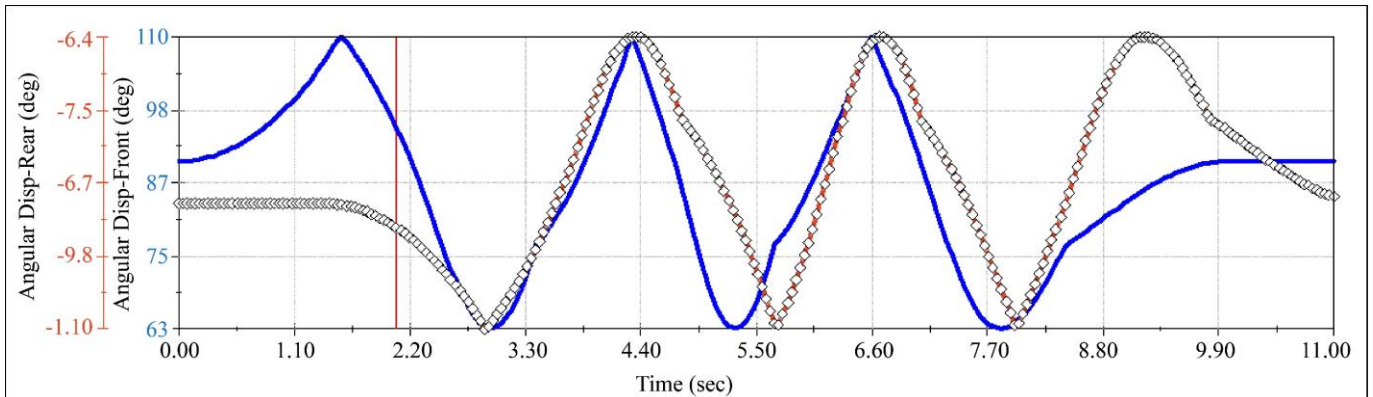


Fig. 22 Angular displacement vs time graph between front and rear legs.

This study is limited to simulation-based validation without experimental implementation; slippage and impact forces are limited.

4. Conclusion

The design and modeling of a quadruped robot is done considering the leg lengths required for the assumed ground clearance. Later, the inverse kinematics have been computed and are clubbed to the required trajectory for an assumed obstacle height of 75mm, which can be varied for the type of motion expected from the robot. Different gaits of quadruped animals have been analyzed, and the required parameters have

been calculated to be given as input for the motion study. The simulations have been done, and the corresponding plots have been generated for each type of gait. The observation of which gait to be applied for which motion is observed as well.

Acknowledgments

We would like to express our gratitude to all the people behind the screen who helped us transform an idea into a real application by providing all the necessary guidance and tools. We are grateful to Dr. S.V. Ramana, Principal, VCE, and the Management of VCE, Hyderabad, for carrying out our dissertation work.

References

- [1] Yunn Lin Hwang, Jung Kuang Cheng, and Van Thuan Truong, "Dynamic Analysis and Control of Industrial Robotic Manipulators," *Applied Mechanics and Materials*, vol. 883, pp. 30-36, 2018. [[CrossRef](#)] [[Google Scholar](#)] [[Publisher Link](#)]
- [2] Sachin Oak, and Vaibhav Narwane, "Design, Analysis and Fabrication of Quadruped Robot with Four Bar Chain Leg Mechanism," *International Journal of Innovative Science, Engineering & Technology*, vol. 1, no. 6, pp. 340-345, 2014. [[Google Scholar](#)] [[Publisher Link](#)]

- [3] Alarazah Hussein Abdulwahab et al., “Quadruped Robots Mechanism, Structural Design, Energy, Gait, Stability, and Actuators: A Review Study,” *International Journal of Mechanical Engineering and Robotics Research*, vol. 12, no. 6, pp. 385-395, 2023. [[CrossRef](#)] [[Google Scholar](#)] [[Publisher Link](#)]
- [4] B. Sandeep, and P. Tamil Selvan, “Design and Development of an Autonomous Quadruped Robot,” *IOP Conference Series: Materials Science and Engineering*, vol. 1012, pp. 1-20, 2021. [[CrossRef](#)] [[Google Scholar](#)] [[Publisher Link](#)]
- [5] M. M. Gor et al., “Development of a Compliant Legged Quadruped Robot,” *Sādhanā*, vol. 43, 2018. [[CrossRef](#)] [[Google Scholar](#)] [[Publisher Link](#)]
- [6] Smita A. Ganjare, V.S Narwane, and Ujwal Deole, “Kinematic Modeling of Quadruped Robot,” *International Journal on Theoretical and Applied Research in Mechanical Engineering*, vol. 2, no. 4, pp. 21-26, 2013. [[Google Scholar](#)] [[Publisher Link](#)]
- [7] Xianbao Chen et al., “Kinematic Analysis And Motion Planning of a Quadruped Robot with Partially Faulty Actuators,” *Mechanism and Machine Theory*, vol. 94, pp. 64-79, 2015. [[CrossRef](#)] [[Google Scholar](#)] [[Publisher Link](#)]
- [8] Claudio Semini et al., “Design of the Hydraulically Actuated Torque-Controlled Quadruped Robot HyQ2Max,” *IEEE/ASME Transactions on Mechatronics*, vol. 22, no. 2, pp. 635-646, 2017. [[CrossRef](#)] [[Google Scholar](#)] [[Publisher Link](#)]
- [9] Jinrong Zhang, Chenxi Wang, and Jianhua Zhang, “The Kinematics Analysis and Configuration Optimize of Quadruped Robot,” *Open Automation and Control Systems Journal*, vol. 6, pp. 1685-1690, 2014. [[CrossRef](#)] [[Google Scholar](#)] [[Publisher Link](#)]
- [10] Gerardo Bleedt et al., “MIT Cheetah 3: Design and Control of a Robust, Dynamic Quadruped Robot,” *2018 IEEE/RSJ International Conference on Intelligent Robots and Systems (IROS)*, Madrid, Spain, pp. 2245-2252, 2018. [[CrossRef](#)] [[Google Scholar](#)] [[Publisher Link](#)]
- [11] Min Sung Kim et al., “Accessorizing Quadrupedal Robots with Wearable Electronics,” *Advanced Intelligent Systems*, vol. 6, no. 4, pp. 1-19, 2024. [[CrossRef](#)] [[Google Scholar](#)] [[Publisher Link](#)]
- [12] Jinrong Zhang, Chenxi Wang, and Jianhua Zhang, “Development of a Pneumatically Actuated Quadruped Robot using Soft–Rigid Hybrid Rotary Joints,” *Robotics*, vol. 13, no. 2, pp. 1-17, 2024. [[CrossRef](#)] [[Google Scholar](#)] [[Publisher Link](#)]
- [13] Yanan Fan et al., “A Review of Quadruped Robots: Structure, Control, and Autonomous Motion,” *Advanced Intelligent Systems*, vol. 6, no. 6, pp. 1-26, 2024. [[CrossRef](#)] [[Google Scholar](#)] [[Publisher Link](#)]
- [14] Nipun Dhananjaya Weerakkodi Mudalige et al., “HyperDog: An Open-Source Quadruped Robot Platform based on ROS2 and Micro-ROS,” *arXiv preprint*, pp. 1-6, 2022. [[CrossRef](#)] [[Google Scholar](#)] [[Publisher Link](#)]
- [15] J.H Shashank Shelke et al., “Smart Quadruped Robot,” *International Research Journal of Engineering and Technology*, vol. 8, no. 6, pp. 208-212, 2024. [[Publisher Link](#)]
- [16] Yam Geva, and Amir Shapiro, “A Novel Design of a Quadruped Robot for Research Purposes,” *International Journal of Advanced Robotic Systems*, vol. 11, no. 7, pp. 1-13, 2014. [[CrossRef](#)] [[Google Scholar](#)] [[Publisher Link](#)]
- [17] V. M. Budanova et al., “MORS: BLDC-based Small Quadruped Robot,” *Journal of Computer and Systems Sciences International*, vol. 63, pp. 983-1007, 2024. [[CrossRef](#)] [[Google Scholar](#)] [[Publisher Link](#)]
- [18] Yunde Shi et al., “Structural Design, Simulation and Experiment of Quadruped Robot,” *Applied Sciences*, vol. 11, no. 22, pp. 1-19, 2021. [[CrossRef](#)] [[Google Scholar](#)] [[Publisher Link](#)]
- [19] Abid Shahriar, and Monim Hasan Anik, “CHIGLU: A Modular Hardware for Stepper Motorized Quadruped Robot — Design, Analysis, Fabrication, and Validation,” *arXiv preprint*, pp. 1-26, 2024. [[CrossRef](#)] [[Google Scholar](#)] [[Publisher Link](#)]
- [20] Marco Hutter et al., “Anymal – A Highly Mobile and Dynamic Quadrupedal Robot,” *2016 IEEE/RSJ International Conference on Intelligent Robots and Systems (IROS)*, pp. 38-44, 2016. [[CrossRef](#)] [[Google Scholar](#)] [[Publisher Link](#)]
- [21] Hamza Khan et al., “Development of the Lightweight Hydraulic Quadruped Robot-MiniHyQ,” *2015 IEEE International Conference on Technologies for Practical Robot Applications (TePRA)*, Woburn, MA, USA, pp. 1-6, 2015. [[CrossRef](#)] [[Google Scholar](#)] [[Publisher Link](#)]
- [22] Pablo Gonzalez de Santos, Elena Garcia, and Joaquin Estremera, *Quadrupedal Locomotion An Introduction to the Control of Four-legged Robots*, SpringerLink, 2016. [[CrossRef](#)] [[Google Scholar](#)] [[Publisher Link](#)]
- [23] Sheng Dong et al., “Gait Planning, and Motion Control Methods for Quadruped Robots: Achieving High Environmental Adaptability: A Review,” *CMES - Computer Modeling in Engineering and Sciences*, vol. 143, no. 1, pp. 1-50, 2025. [[CrossRef](#)] [[Google Scholar](#)] [[Publisher Link](#)]
- [24] Mauricio Becerra-Vargas, and Eduardo Paciência Godoy, “Model-Based Control Implementation of Quadruped Robots With MuJoCo,” *IEEE Access*, vol. 13, pp. 144770-144784, 2025. [[CrossRef](#)] [[Google Scholar](#)] [[Publisher Link](#)]
- [25] E.R. Westervelt, J.W. Grizzle, and D.E. Koditschek, “Hybrid Zero Dynamics of Planar Biped Walkers,” *IEEE Transactions on Automatic Control*, vol. 48, no. 1, pp. 42-56, 2003. [[CrossRef](#)] [[Google Scholar](#)] [[Publisher Link](#)]